View metadata, citation and similar papers at core.ac.uk
brought to you by CORE
provided by CiteSeerX


International Electrical Engineering Journal (IEEJ)
Vol. 3 (2012) No. 2, pp. 738-744
ISSN 2078-2365

# Capacitors Natural Voltage Balancing Mechanism Investigation in Flying Capacitor Multicell Converters

*Vahid Dargahi and Abbas Shoulaie*

*Department of Electrical Engineering, Iran University of Science and Technology, Tehran 16846, Iran*

*vdargahi@elec.iust.ac.ir, shoulaie@iust.ac.ir*

*Abstract*—**This paper presents an analytical analysis of flying capacitors voltage balancing process in flying capacitor multicell converters. The analysis is based upon renowned theory of Double Fourier series which leads to modeling and state-space representation of converters. State-space representation of converter can be utilized to investigate the transient and steady states of internal flying capacitors voltages. To provide verification, experimental results acquired from a laboratory prototype are compared against numerical solution of differential equations of converter state-space representation and simulation results.**

***Keywords Flying Capacitor Multicell Converter, Double Fourier Series, Self balancing.***

## I. INTRODUCTION

As a consequence of reaching higher power and lack of its suitable ranged switches, multilevel converters popped up in 1975 and have been continuously developed in recent years due to the necessity of increase in power level of industrial applications especially high power applications such as high power AC motor drives, active power filters, reactive power compensation and FACTS devices. The main reason is the capability of these topologies to handle voltage/power in the range of kilovolts/megawatts as a result of recent developments in the area of high power semiconductors [1]-[5].

The concept of multilevel arises from acquiring a staircase output voltage waveform as voltage levels from input dc voltages by means of converter appropriate configuration and its proper switching pattern. This staircase voltage by its resemblance to sinusoidal voltage waveform leads to primitive advantages of utilizing switches with low-voltage ratings, higher power quality, lower total harmonic distortion, etc [1]-[5].

The term multilevel starts with the three-level converter introduced by Nabae *et al.* The Neutral Point Clamped (NPC) converter, presented in the early 80's, is a standard topology in industry on its 3-level version. However, for a higher number of levels, this topology has some drawbacks such as: voltage balance of the dc-link capacitors and the number of clamping diodes [2]-[4].

Alternatives for the NPC converters are the multicell topologies. Different cells and approaches to interconnect them lead to many topologies which the most important ones are the Cascaded Multicell (CM) and the Flying Capacitor Multicell (FCM) accompanied by its sub-topology Stacked Multicell (SM) converters [2][3][5].

The FCM converter, and its derivative, the SM converter, have many advantageous properties for medium voltage applications, particularly the transformer-less operation and the ability to naturally maintain the flying capacitors voltages at their target operating levels. This substantial property is called natural balancing and allows the construction of such converters with a large number of voltage levels. Natural self-balancing of the flying capacitors voltages occurs without any feedback control. A necessary condition for this phenomenon is that average currents of the flying capacitors must be zero. As a result, each cell must be controlled with the same duty cycle and a regular phase shifted progression along the cells. Generally, an output *RLC* filter (balance booster circuit), tuned to the switching frequency or multiple of that, is suggested to be connected across the load in order to accelerate this self balancing process in the transient states [2][3][5].

The FCM converter uses a series connection of "cells" comprising a flying capacitor and its associated complimentary switch pair and produces a switched voltage that is the sum of the individual cell states [2][3][5].

Despite of mentioned appreciable advantages, multilevel converters possess some following main drawbacks: increased number of isolated dc voltages, clamping diodes, capacitors and of power semiconductor switches accompanied by their related gating and protection circuits which result in a sophisticated overall system [2][3][5].

As mentioned, voltage natural balancing mechanism is a fundamental principle in flying capacitor and stacked multicell converters which consents to construction of voltage levels at the converter output [8]-[11]. The main objective of this paper is to provide a mathematical model for flying capacitor multicell converters intended for investigation of transient and steady state of flying capacitors voltages accompanied by taking into account the effect of balance booster circuit.

International Electrical Engineering Journal (IEEJ)
Vol. 3 (2012) No. 2, pp. 738-744
ISSN 2078-2365

## II. INSTANTANEOUS MODELING OF FLYING CAPACITOR MULTICELL CONVERTERS IN STATE-SPACE REPRESENTATION

### A. *Fundamental Concepts of Flying Capacitors Multicell Converters*

Flying capacitor multicell converters (FCMCs) which have been proposed by T.A. Meynard are relatively new breed of multilevel converters in comparison with conventional neutral point clamped (NPC) and cascade H-bridge (CHB) ones. A typical configuration of FCMC is depicted in Fig 1. As illustrated, *R* cells in a FCMC are overlapped to form a required converter's leg. Each cell consists of one voltage source (a dc voltage source equal to E in *R*th cell and capacitors possessing specific voltages in remaining cells) and two power semiconductor switches which are in complementary state to each other to avoid short-circuiting of voltage sources. Phase shifted carrier sinusoidal pulse width modulation (PSCSPWM) technique is the most common control scheme which is applied to switching strategy of FCMCs to guaranty both best harmonic performance and voltage balancing mechanism of flying capacitors. It should be noted that in a *R*-cell FC converter each switch sustains just a fraction of DC link voltage, i.e. *E/R*. This *R*-cell configuration leads to *R*+1 levels of voltage with peak to peak voltage value of *E* at the converter output. Flying capacitor multicell converters are in preference to the NPC and CHB ones as considering advantages such as: modularity, non-interdependency of cells as fault occurs and ease of reaching higher voltage levels just by introducing new cells [2][3][5].

Switches states of a 4-cell-5-level FCMC and output voltage, using PSCSPWM control method, are illustrated in Table-1.

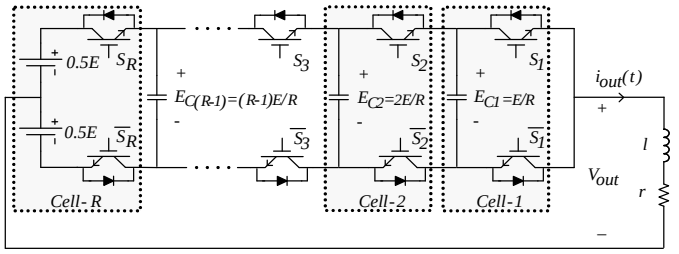


Fig. 1. *R*-cell flying capacitor multicell converter with maximum output voltage value of *E*.

Table-1: States of switches in a 4-cell-5-level conventional FCMC.

| **Output Voltage** | **State of Switches** {($S_4$, $S_3$, $S_2$, $S_1$)} | **Number of States** |
|---|---|---|
| *+E* | {(1,1,1,1)} | 1 |
| *+0.5E* | {(1,1,1,0)(1,1,0,1)(1,0,1,1) (0,1,1,1)} | 4 |
| *0* | {(1,1,0,0)(1,0,0,1)(0,0,1,1)(1,0,1,0)(0,0,1,1)(0,1,0,1)} | 6 |
| *-0.5E* | {(1,0,0,0)(0,1,0,0)(0,0,1,0)(0,0,0,1)} | 4 |
| *-E* | {(0,0,0,0)} | 1 |

The output voltage of a *R*-cell FC converter has *R+1*-levels and its frequency spectrum has the harmonics around the $(R\times k\times f_{sw})$ th harmonic where *k* and $f_{sw}$ are the integer number and the switching frequency, respectively [2][3][5].

### B. *Instantaneous Model of the Converter in the State-Space Representation*

By utilizing proper switching pattern in FCMCs, their capacitor voltages would reach to the specific values which allow to constructing the desired output voltage levels. This property is known as natural voltage balancing mechanism and is achieved using phase shifted carrier pulse width modulation (PSCPWM) switching technique in the converter [8]-[11].

Natural self-balancing process of the flying capacitors voltages, as one of the advantages of FCM converters occurs without any feedback control. A necessary condition for this phenomenon is that average currents of the flying capacitors must be zero. As a result, each cell must be controlled with the same duty cycle and a regular phase shifted progression along the cells. Generally, an output *RLC* filter (balance booster circuit), tuned to the switching frequency or multiple of that, is suggested to be connected across the load in order to accelerate this self balancing process in the transient states. In this case, the dynamic of the self-balancing process depends on the impedance of load at the switching frequency. If the impedance at the switching frequency is high then the natural balancing is very slow and vice versa. The output *RLC* filter should be tuned to the switching frequency as follow [8]-[11]:

$$\sqrt{L_b \cdot C_b} = \frac{1}{2 \cdot \pi \cdot f_{sw}} \qquad (1)$$

Where, $f_{sw}$ is the switching frequency, $L_b$ and $C_b$ are inductance and capacitance of the output *RLC* booster circuit, respectively.

However in this section a mathematical model of the converter will be presented to verify this balancing property. This model describes time domain differential equations of the flying capacitors voltages and state-space representation of the converter. Utilization a numerical solution of differential equations leads to acquire transient and steady state response of flying capacitors voltages. According to Fig. 1, a switching function of a cell $\rho$ is defined as follows [8]-[11]:

$$H_\rho(t) = \begin{cases} +1 & if \;\; S_\rho \;\; is\, on \\ -1 & if \;\; S_\rho \;\; is\, off \end{cases} \qquad \rho = 1:R \qquad (2)$$

And its double Fourier series expansion can be expressed as follows [6]-[7]:

International Electrical Engineering Journal (IEEJ)
Vol. 3 (2012) No. 2, pp. 738-744
ISSN 2078-2365

$$H_\rho(t) = M\cos(\omega_r t+\phi_r) + \sum_{m=1}^{\infty}\sum_{n=-\infty}^{\infty}\left(\begin{array}{l}\frac{4}{m\pi}\sin\left(\left[m+n\right]\frac{\pi}{2}\right)J_n\left(m\frac{\pi}{2}M\right)\times \\ \cos\left(m\left[\omega_c t+\phi_c+\frac{(\rho-1)2\pi}{R}\right]+n\left[\omega_r t+\phi_r\right]\right)\end{array}\right) \quad (3)$$

Where $M$, $\omega_r$, $\phi_r$, $J_n(.)$, $\omega_c$, $\phi_c$ are modulation index, angular frequency of reference sinusoidal waveform, phase angle of reference sinusoidal waveform, *n*th order Bessel function of first kind, triangular carrier waveform angular frequency and triangular carrier waveform phase angle, respectively.

Output voltage and current of the converter and associated differential equations of the flying capacitors voltages based on mentioned switching functions can be obtained as follows [8]-[11]:

$$V_{out} = \frac{E}{2}H_R(t)+\frac{1}{2}\sum_{\rho=1}^{R-1}\left[\left(H_\rho(t)-H_{\rho+1}(t)\right)\right]E_{c\rho} \quad (4)$$

$$i_{out}(t) = \frac{V_{out}(t)}{Z_L} \quad (5)$$

$$C_\rho\frac{dE_{c\rho}}{dt} = \frac{1}{2}\left[H_{\rho+1}(t)-H_\rho(t)\right]i_{out}(t) \quad (6)$$

Where, $Z_L$ is a series connection of resistance $(r)$ and inductance $(l)$ and $C_\rho$ is capacitance of flying capacitors. Flying capacitor multicell converter's state-space representation can be written as follows:

$$\dot{E}_c = A\times E_c + B\times E \quad (7)$$

$$E_c = \left[E_{c1}\ \ E_{c2}\ \ E_{c3}.....E_{c(R-1)}\right]^T \quad (8)$$

$$A_{ij} = \frac{-1}{4C_i}\left[H_{i+1}(t)-H_i(t)\right]\left[\lambda_{j+1}(t)-\lambda_j(t)\right] \quad i,j=1:R-1 \quad (9)$$

$$\boldsymbol{B}_{i1} = \frac{\lambda_R(t)}{4C_i}\left[H_{i+1}(t)-H_i(t)\right] \quad i=1:R-1 \quad (10)$$

And:

$$\lambda_\rho(t) = \frac{H_\rho(t)}{Z_L} = \frac{M}{\sqrt{\left(r^2+(\omega_r l)^2\right)}}\cos\left(\omega_r t+\phi_r-\tan^{-1}\left(\frac{\omega_r l}{r}\right)\right) + \sum_{m=1}^{\infty}\sum_{n=-\infty}^{\infty}\left(\begin{array}{l}\frac{4}{m\pi\sqrt{\left(r^2+\left((m\omega_c+n\omega_r)l\right)^2\right)}}\sin\left(\left[m+n\right]\frac{\pi}{2}\right)\times \\ J_n\left(m\frac{\pi}{2}M\right)\cos\left(\begin{array}{l}m\left[\omega_c t+\phi_c+\frac{(\rho-1)2\pi}{R}\right] \\ +n\left[\omega_r t+\phi_r\right] \\ -\tan^{-1}\left(\frac{(m\omega_c+n\omega_r)l}{r}\right)\end{array}\right)\end{array}\right) \quad (11)$$

$\rho = 1:R$

To consider the balance booster circuit effect on the dynamic of the self-balancing process following modification should be applied to the acquired state-space equations:

$$A_{ij} = \frac{-1}{4C_i}\left[H_{i+1}(t)-H_i(t)\right]\left[\left(\lambda_{j+1}(t)+\lambda'_{j+1}(t)\right)-\left(\lambda_j(t)+\lambda'_j(t)\right)\right] \quad (12)$$

$i,j=1:R-1$

$$\boldsymbol{B}_{i1} = \frac{1}{4C_i}\left[\lambda_R(t)+\lambda'_R(t)\right]\left[H_{i+1}(t)-H_i(t)\right] \quad (13)$$

$i=1:R-1$

And:

International Electrical Engineering Journal (IEEJ)
Vol. 3 (2012) No. 2, pp. 738-744
ISSN 2078-2365

$$\lambda'_{\rho}(t)=\frac{H_{\rho}(t)}{Z_b}$$

$$=\frac{M}{\sqrt{\left(R_b{}^2+\left(\omega_r L_b-\left(\omega_r C_b\right)^{-1}\right)^2\right)}}\cos\left(\begin{array}{l}\omega_r t+\phi_r\\-\tan^{-1}\left(\dfrac{\omega_r L_b-\left(\omega_r C_b\right)^{-1}}{R_b}\right)\end{array}\right)$$

$$+\sum_{m=1}^{\infty}\sum_{n=-\infty}^{\infty}\left(\begin{array}{l}\dfrac{4}{m\pi\sqrt{\left(R_b{}^2+\left(\left(m\omega_c+n\omega_r\right)L_b-\left(\left(m\omega_c+n\omega_r\right)C_b\right)^{-1}\right)^2\right)}}\times\\\sin\left(\left[m+n\right]\dfrac{\pi}{2}\right)J_n\left(m\dfrac{\pi}{2}M\right)\times\\\cos\left(\begin{array}{l}m\left[\omega_c t+\phi_c+\dfrac{(\rho-1)2\pi}{R}\right]\\+n\left[\omega_r t+\phi_r\right]\\-\tan^{-1}\left(\dfrac{\left(m\omega_c+n\omega_r\right)L_b-\left(\left(m\omega_c+n\omega_r\right)C_b\right)^{-1}}{R_b}\right)\end{array}\right)\end{array}\right) \quad (14)$$

$$\rho=1:R$$

## III. Numerical and Simulation Results

To provide verification to the elaborated state-space representation of the FCMC, numerical solution is utilized to solve differential equations of 6-cell-7-level and 4-cell-5-level converters. Transient and steady state of internal flying capacitors voltages of mentioned converters acquired from state-space numerical solution are shown in Figs. 2-6. System parameters used in numerical solution are given in Tables 2-5.

Table-2: Parameters used in simulation and numerical solution of state-space representation of 6-cell-7-level FCMC.

| System Parameters | Values |
|---|---|
| DC voltage (*E*) | 600 V |
| Internal flying capacitors (*C*) | 560 uF |
| PS-SPWM carrier frequency ($f_{SW}$) | 5 kHz |
| Fundamental output voltage frequency | 50 Hz |
| Modulation index | 0.8 |
| Resistive-inductive load (*r-l*) | 10 Ω – 50 mH |
| Booster circuit(*RLC*) | 20 Ω – 10 uH-101.32 uF |

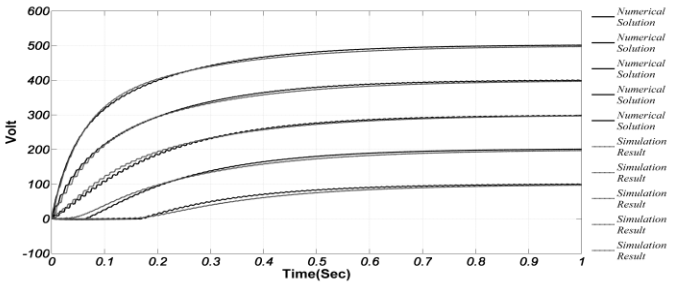


Fig. 2. Transient and steady state of internal flying capacitors voltages of a 6-cell-7-level FCMC acquired from state-space numerical solution and simulation for resistive-inductive load in parallel with *RLC* booster circuit.

Table-3: Parameters used in simulation and numerical solution of state-space representation of 6-cell-7-level FCMC.

| System Parameters | Values |
|---|---|
| DC voltage (*E*) | 600 V |
| Internal flying capacitors (*C*) | 2200 uF |
| PS-SPWM carrier frequency ($f_{SW}$) | 5 kHz |
| Fundamental output voltage frequency | 50 Hz |
| Modulation index | 0.8 |
| Resistive-inductive load (*r-l*) | 10 Ω – 50 mH |
| Booster circuit(*RLC*) | 10 Ω – 10 uH-101.32 uF |

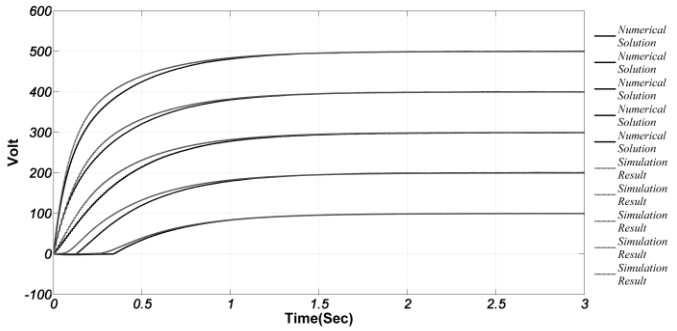


Fig. 3. Transient and steady state of internal flying capacitors voltages of a 6-cell-7-level FCMC acquired from state-space numerical solution and simulation for resistive-inductive load in parallel with *RLC* booster circuit.

Table-4: Parameters used in simulation and numerical solution of state-space representation of 4-cell-5-level FCMC.

| System Parameters | Values |
|---|---|
| DC voltage (*E*) | 600 V |
| Internal flying capacitors (*C*) | 2200 uF |
| PS-SPWM carrier frequency ($f_{SW}$) | 5 kHz |
| Fundamental output voltage frequency | 50 Hz |
| Modulation index | 0.8 |
| Resistive-inductive load (*r-l*) | 10 Ω – 50 mH |
| Booster circuit(*RLC*) | 10 Ω – 10 uH-101.32 uF |

International Electrical Engineering Journal (IEEJ)
Vol. 3 (2012) No. 2, pp. 738-744
ISSN 2078-2365

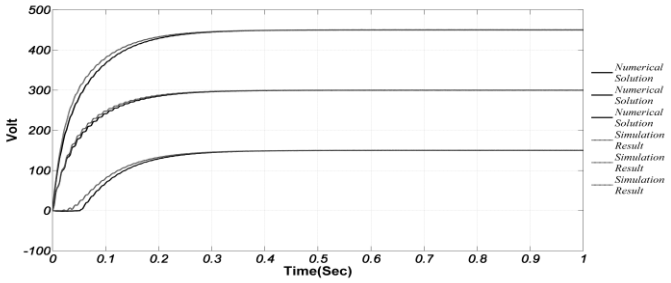


Fig. 4. Transient and steady state of internal flying capacitors voltages of a 4-cell-5-level FCMC acquired from state-space numerical solution and simulation for resistive-inductive load in parallel with *RLC* booster circuit.

Table-5: Parameters used in simulation and numerical solution of state-space representation of 4-cell-5-level FCMC.

| System Parameters | Values |
|---|---|
| DC voltage (*E*) | 600 V |
| Internal flying capacitors (*C*) | 2200 uF |
| PS-SPWM carrier frequency ($f_{SW}$) | 5 kHz |
| Fundamental output voltage frequency | 50 Hz |
| Modulation index | 0.9 |
| Resistive-inductive load (*r-l*) | 10 Ω – 50 mH |
| Booster circuit(*RLC*) | 10 Ω – 10 uH-101.32 uF |

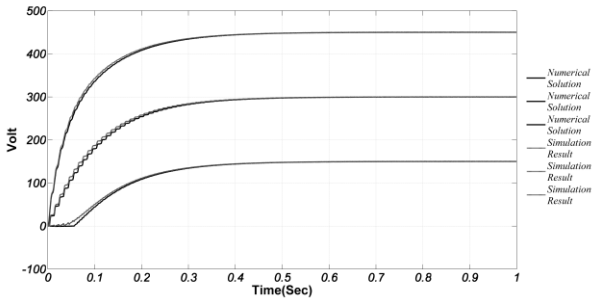


Fig. 5. Transient and steady state of internal flying capacitors voltages of a 4-cell-5-level FCMC acquired from state-space numerical solution and simulation for resistive-inductive load in parallel with *RLC* booster circuit.

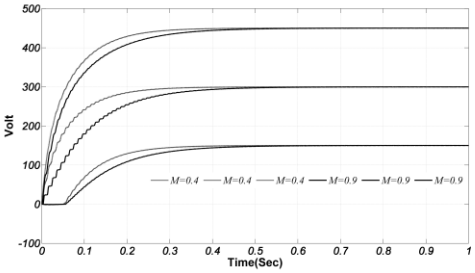


Fig. 6. Transient and steady state of internal flying capacitors voltages of a 4-cell-5-level FCMC acquired from state-space numerical solution and simulation for resistive-inductive load in parallel with *RLC* booster circuit for two different modulation indexes.

Numerical solutions are in accordance with simulation results and admit the model of the converter. It is worthwhile noting that the value of resistor in the balance booster circuit plays an important role in transient state of flying capacitors voltages and its reduction accelerates the self balancing process in flying capacitors and vice versa.

## IV. EXPERIMENTAL RESULTS

To verify the mathematical model of FCMC, the measured transient and steady state voltages of flying capacitors of a 3-cell-4-level converter acquired from the prototype system, illustrated in Fig. 7 and Fig. 9, are compared against simulation results and numerical solution of the converter time-domain differential equations, presented in Fig. 8 and Fig.10. Also main parameters of the converter are given in Tables 6 and 7. The match between simulation, numerical solution and experimental results confirms the modified mathematical model of FCMC.

Table-6: Parameters used in simulation, numerical solution, and experimental converter.

| System Parameters | Values |
|---|---|
| DC voltage (E) | 75 V |
| Internal flying capacitors (C) | 560 uF |
| PS-SPWM carrier frequency ($f_{SW}$) | 5 kHz |
| Fundamental output voltage frequency | 50 Hz |
| Modulation index | 0.8 |
| Resistive-inductive load ($R_L$- $L_L$) | 25 Ω – 30 mH |
| Booster circuit | 24 Ω – 10 uH- 101.32 uF |

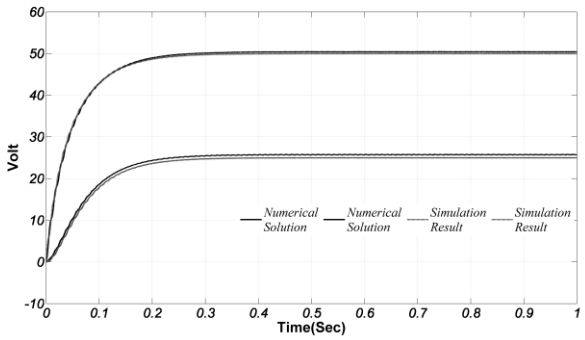


Fig. 7. Transient and steady state of internal flying capacitors voltages of a 3-cell-4-level FCMC acquired from state-space numerical solution and simulation for resistive-inductive load in parallel with *RLC* booster circuit.

International Electrical Engineering Journal (IEEJ)
Vol. 3 (2012) No. 2, pp. 738-744
ISSN 2078-2365

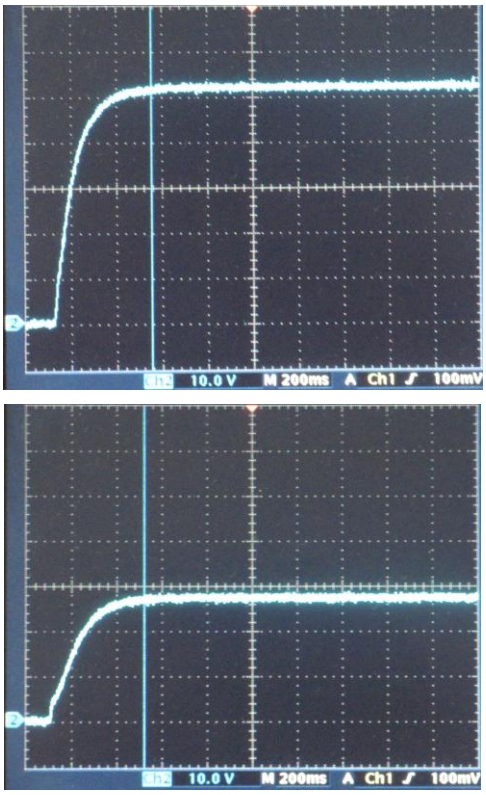


Fig. 8. Transient and steady state of internal flying capacitors voltages of a 3-cell-4-level FCMC acquired from experimental prototype for resistive-inductive load in parallel with *RLC* booster circuit.

Table-7: Parameters used in simulation, numerical solution, and experimental converter.

| System Parameters | Values |
|---|---|
| DC voltage (E) | 75 V |
| Internal flying capacitors (C) | 560 uF |
| PS-SPWM carrier frequency ($f_{SW}$) | 5 kHz |
| Fundamental output voltage frequency | 50 Hz |
| Modulation index | 0.8 |
| Resistive-inductive load ($R_L$- $L_L$) | 25 Ω – 30 mH |
| Booster circuit | 24 Ω – 10 uH- 101.32 uF |

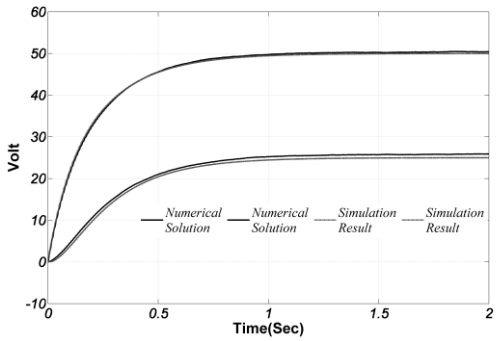


Fig. 9. Transient and steady state of internal flying capacitors voltages of a 3-cell-4-level FCMC acquired from state-space numerical solution and simulation for resistive-inductive load in parallel with *RLC* booster circuit.

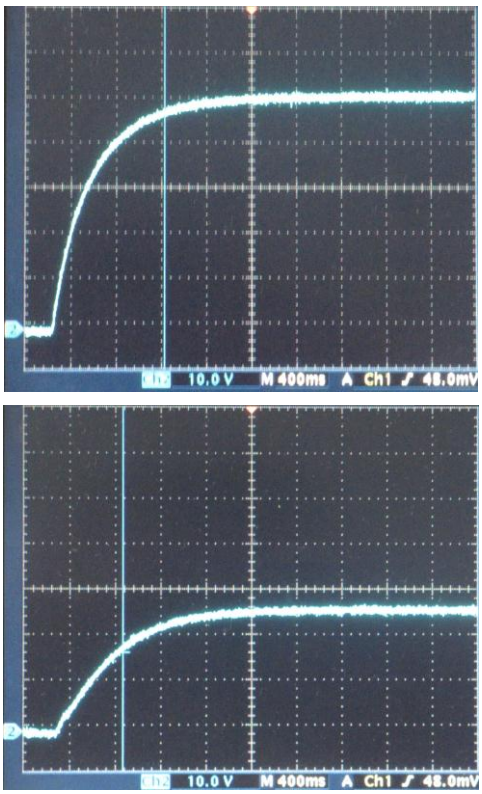


Fig. 10. Transient and steady state of internal flying capacitors voltages of a 3-cell-4-level FCMC acquired from experimental prototype for resistive-inductive load in parallel with *RLC* booster circuit.

## V. CONCLUSION

Multicell converters are very interesting for high-power/medium-voltage applications, for considerably improvement of the output voltage frequency spectrum and reduction of the conduction losses, switching ripple and value of *dV/dt*.

This paper presents a modified mathematical model of flying capacitor multicell converters. In the proposed model the effect of balance booster circuit which is usually connected in parallel with load to accelerate the self balancing process of flying capacitors, is also considered. Numerical solutions, simulation and experimental results are in accordance with each other and confirm the validity of proposed model for FCMCs.

## REFERENCES

[1] R. H. Baker and L. H. Bannister, “Electric power converter,” U.S. Patent 3 867 643, Feb. 1975.

[2] J. S. Lai and F. Z. Peng, "Multilevel converters—A new breed of power converters," in *Proc. IEEE Ind. Applicat. Soc. Annu. Meeting*, 1995, pp. 2348–2356.

[3] J. Rodriguez, J. Lai, and F. Z. Peng, "Multilevel inverters: A survey of topologies, controls and applications," *IEEE Trans. Ind. Electron.*, vol. 49, no. 4, pp. 724–738, Aug. 2002.

[4] A. Nabae, I. Takahashi, and H. Akagi, "A new neutral-point clamped PWM inverter," *IEEE Trans. Ind. Applicat.*, vol. IA-17, pp. 518–523, Sept./Oct. 1981.

[5] T. A. Meynard and H. Foch, "Multi-level choppers for high voltage applications," *Eur. Power Electron. Drives J.*, vol. 2, no. 1, p. 41, Mar. 1992.

[6] H. S. Black, *Modulation Theory*. New York: Van Nostrand, 1953.

[7] D. G. Holmes and T. A. Lipo, Pulse Width Modulation for Power Converters: Principles and Practice. Piscataway, NJ: IEEE Press, 2003.

[8] X. Yuan, H. Stemmler, and I. Barbi, "Self-balancing of the clampingcapacitor- voltages in the multilevel capacitor-clamping-inverter under sub-harmonic PWM modulation," *IEEE Trans. Power Electron.*, vol. 16, no. 2, pp. 256–263, Mar. 2001.

[9] R.Wilkinson, H. du Mouton, and T. Meynard, "Natural balance of multicell converters : The two-cell case," *IEEE Trans. Power Electron.*, vol. 21, no. 6, pp. 1649–1657, Nov. 2006.

[10] R.Wilkinson, H. du Mouton, and T. Meynard, "Natural balance of multicell converters: The general case," *IEEE Trans. Power Electron.*, vol. 21, no. 6, pp. 1658–1666, Nov. 2006.

[11] B. P. McGrath and D. G. Holmes, "Analytical modelling of voltage balance dynamics for a flying capacitor multilevel converter," in *Conf. Rec. IEEE Power Electron. Specialists Conf. (PESC)*, 2007, pp. 968–974.